CrossMark
click for updates

Exploring the pressure–temperature behaviour of crystalline and plastic crystalline phases of N-isopropylpropionamide†

R. Quesada-Cabrera,[a] Y. Filinchuk,[b] P. F. McMillan,[a] E. Nies,[c] V. Dmitriev[d] and F. Meersman*[ae]

The phase behaviour of crystalline and plastic crystalline phases of N-(isopropyl)propionamide (NiPPA) has been investigated by X-ray diffraction and a tentative P,T diagram has been constructed. The observed phase transitions are highly dependent on kinetics, and metastable co-existence of both phases can be observed. At lower pressures (up to 400 MPa) the plastic crystalline phase transforms into the crystalline phase as observed for other plastic crystalline systems, although the slopes (dT/dP) for both the liquid-to-plastic crystal and plastic crystal-to-crystal transitions are both positive and likely to run nearly parallel to each other. Higher pressures result in a highly anisotropic deformation of the crystal packing and at around 4 GPa the NiPPA crystals undergo a isosymmetric phase transition. An instability is observed at 350 K and 1400 MPa where the crystalline X-ray diffraction pattern is lost during heating accompanied by a rapid drop in pressure of the cell. This may correspond to a melting event characterised by a negative dT_m/dP slope.

Introduction

Compression of solids or liquids can be used to gain insight into the state of matter and the underlying intra- and intermolecular interactions. This approach can be applied to interrogate both small molecular systems and large biological macromolecules that can be in the solid state or in solution.[1,2] In the case of molecular solids pressure offers an attractive method to search for potential polymorphs that are relevant for, for instance, pharmaceutical applications.[2,3] Exposure of solids to high pressures may also provide information on the compression of intermolecular interactions and how these influence the response of the molecular packing to pressure.[3–6] For example, in layered structures such as paracetamol anisotropic compression is observed due to the presence of weak van der Waals interactions between the layers and less compressible hydrogen bonds linking the molecules within the layer.[4] Hydrogen bonds have also been thought to be responsible, at least partly, for the absence of any phase transitions in e.g. pyridinium nitrate and acetaminophen, in a pressure range where comparable molecules without hydrogen bonds do undergo a pressure-induced polymorphous transition.[5,7,8]

Molecular systems can display a wide variety of solid phases, including crystalline polymorphs and plastic crystals.[2,9–11] The latter are also referred to as orientationally disordered states as they are characterized by a crystal-like positional order and a rotational disorder of molecular units. Apart from practical applications, plastic crystalline phases may also serve as model systems for structural glass formers.[12] Indeed, plastic crystalline phases are considered to be strong to intermediate glass formers. An example of a molecular system that undergoes a crystal to plastic crystalline phase transition upon heating is N-(isopropyl)propionamide (NiPPA). This small organic molecule contains both hydrogen bond donor and acceptor groups. Its phase behavior in aqueous solution could be related to that of its polymer counterpart, the thermoresponsive water-soluble poly(N-isopropylacrylamide) (PNiPA).[13,14] In its pure form it was found to crystallize from the melt into a plastic crystalline phase with a tetragonal unit cell at 324 K.[15] At lower temperatures a transition to a crystalline form was observed (T_m = 284 K). The crystalline phase is characterized by a primitive monoclinic cell (a = 17.4621(16) Å, b = 8.9077(13) Å, c = 4.9399(5) Å) at 278 K and 0.1 MPa.

[a] Christopher-Ingold Laboratories, Department of Chemistry, University College London, 20 Gordon Street, WC1H 0AJ, London, UK. E-mail: f.meersman@ucl.ac.uk
[b] Institute of Condensed Matter and Nanosciences (IMCN), Université Catholique de Louvain, Place L. Pasteur 1, bte L4.01.03, B-1348 Louvain-la-Neuve, Belgium
[c] Division of Molecular and Nanomaterials, Department of Chemistry, Katholieke Universiteit Leuven, Celestijnenlaan 200F, B-3001, Leuven, Belgium
[d] Swiss-Norwegian Beam Lines, European Synchrotron Radiation Facilities, BP 220, F-38043 Grenoble Cedex, France
[e] Biomolecular & Analytical Mass Spectrometry group, Department of Chemistry, University of Antwerp, Groenenborgerlaan 171, B-2020 Antwerp, Belgium
† Electronic supplementary information (ESI) available: Crystallographic data of NIPPA up to 10 GPa. Diffraction patterns of the plastic crystalline phase and Rietveld refinements of the crystalline phase at 0.1 MPa and 6 GPa. See DOI: 10.1039/c5ce00032g

These experiments on NiPPA were all performed as a function of temperature at atmospheric pressure. To further investigate the solid state behavior pressure is used as an additional perturbation parameter. Previously investigated plastic crystalline–crystalline transitions under pressure include *n*-alkanes, cyclopentane, *tert*-butyl compounds, 2,2-dimethylpropane and 2-methyl-2-chloropropane.[16–20] Of the *tert*-butyl compounds, both pivalic acid and neopentyl alcohol contain hydrogen bonds.[19] As pointed out above the presence of hydrogen bonds may introduce specific pressure–temperature behavior. Moreover, the number of high pressure studies on plastic crystalline systems that contain hydrogen bonds remains limited. These systems were investigated by various techniques including Raman spectroscopy, differential thermal analysis and crystallography. Here synchrotron X-ray diffraction has been employed to study the pressure–temperature (*P*,*T*) behavior of NiPPA *in situ* using a diamond anvil cell. The sample was first subjected to pressures in the GPa range at room temperature in order to establish the pressure behaviour of its crystalline phase and to explore any new solid–solid phase transitions. In the second part of the study pressures in the order of a few 100 MPa are applied to map the *P*,*T* phase diagram of NIPPA, particularly exploring the plastic crystalline to crystalline transition under pressure at various temperatures. The result is a first view of the stable and metastable NiPPA phase transformation behaviour that covers a wider pressure range (up to 10 GPa) than has been explored for most other plastic crystalline molecular systems.[19,20] It reveals complex behaviour with an isosymmetric phase transition of the crystalline phase occurring above 4 GPa, transformation between the plastic (PC), crystalline (C) and liquid phases between 1 atm and 200 MPa, and a crystal instability that may be associated with melting in the 300–1400 MPa range. The volume change associated with the crystalline to plastic crystalline phase transition is determined for the first time.

Experimental section

NiPPA was obtained following the synthesis described elsewhere.[13] Pressure experiments were performed using a Mao–Bell type diamond anvil cell (DAC) with 600 μm diameter culets. The sample was contained within the anvils in a laser-drilled (∅300–400 μm) stainless steel gasket, either in non-hydrostatic conditions or immersed in a suitable pressure–transmitting medium (silicone oil) that provided a hydrostatic environment. *In situ* pressure measurements were carried out by the ruby fluorescence method.[21] The ruby scale for the *in situ* determination of pressure in the DAC at high temperature was corrected according to Rekhi *et al.*[22]

Synchrotron powder X-ray diffraction (XRD) data were obtained at the Swiss-Norwegian Beam Lines (SNBL, BM01A) at ESRF (Grenoble, France). The beam energy was ~17 keV (λ = 0.71171 Å) and the beam size at the sample was 100 × 100 μm^2. The detector parameters and the wavelength were calibrated with a standard sample of LaB$_6$ from NIST. Data were collected using a MAR345 image plate detector. Data integration was carried out using the Fit2D software.[23] The refinement of the patterns was carried out using the FullProf program.[24] Further details of the analysis of the XRD data are described elsewhere.[15] The temperature studies were carried out using an Oxford Cryostream 700+ and the temperature was monitored with type K thermocouples.

Results and discussion

Compression of the crystalline phase

Fig. 1 shows the effect of pressures up to 10.3 GPa on the X-ray diffraction (XRD) pattern of the crystalline phase of NiPPA. The sample was loaded using silicone oil as pressure–transmitting medium. The XRD pattern at 0.1 GPa corresponds to the known monoclinic $P2_1/a$ structure.[15] Note that at this temperature (293 K) NiPPA normally adopts a plastic crystalline state when cooled from the melt. However, as the sample was left at room temperature for a considerable amount of time (months) it transformed into its thermodynamically stable crystalline state before the X-ray diffraction data were obtained. That result highlights the kinetic issues associated with determining polymorphic phase transitions in this material. The initial compression steps up to 1 GPa show a large shift in the peak positions and a splitting of the peak at 10.2°, that initially arises from the overlap of three reflections (planes [1,1,1],[2,1,−1] and [2,0,1]). The peak shifts upon compression are shown also in Fig. 1. Further compression induces significant changes in the 8–12° region of the patterns, apart from the expected intensity drop and broadening of all reflections due to increasing structural disorder. However, all patterns still could be refined using the initial monoclinic $P2_1/a$ model, although the refinements do reveal interesting changes in the crystal structure.

The crystal is anisotropically compressed, mainly along the *a* axis that has undergone a shortening by about 20% at 10 GPa. In contrast, the length of the *b* and *c* axes is only reduced by 5% at the maximum pressure (Fig. 2). This is consistent with earlier studies that showed that the strain induced in low-symmetry molecular crystals is usually highly anisotropic. In layered structures, it often correlates with the stacking directions, maximum compressibility being observed normal to the layers.[4] This is also the case here. Even though it may seem expected, this is not always so. Examples of the opposite behaviour include dimedone and benzoquinone.[8] In addition to the cell length parameters there are also changes in the orthorhombic angle that opens up a few degrees and in the cell volume that is reduced by 30% upon compression (Fig. 2).

The data suggest that the compound undergoes an anisotropic distortion rather than a phase transition. The latter statement is based on the continuous curvature observed for the cell volume as a function of pressure. However, at high pressures the intermolecular O⋯O distances (*d*) come close to the N⋯O intermolecular separation, corresponding to the H-bond distance (Fig. 3(a)). When plotting the change in
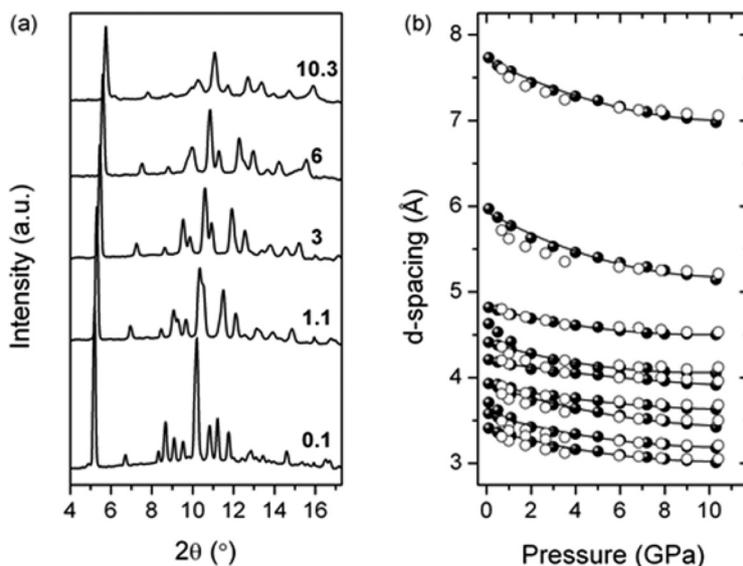
Fig. 1 Selected X-ray diffraction patterns of the crystalline phase of NiPPA (a) and peak shifts upon compression at 293 K (b). Pressure values are given in GPa. The empty symbols in (b) correspond to d-spacings during decompression.

O···O distance upon compression, a sudden jump in the curve is observed between 4 and 5 GPa (Fig. 3), beyond which the compression behaviour is linear with $\partial d/\partial P = -0.034 \pm 8 \times$
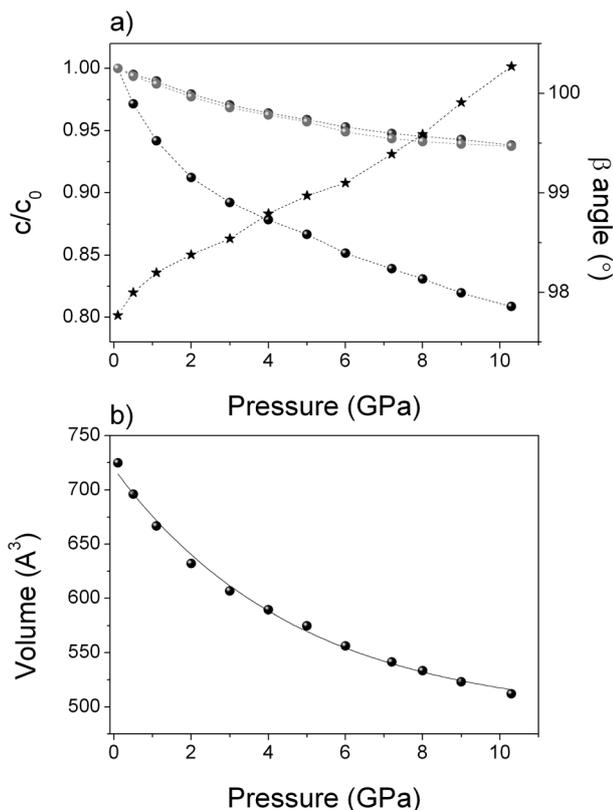

Fig. 2 Normalised cell parameters (a) and cell volume (b) of the crystalline phase upon compression. Length variation of the a axis (black symbols), b axis (dark grey symbols) and c axis (grey symbols) and the change in orthorhombic angle β (stars).

10^{-4} Å GPa^{-1}. The existing H-bond distance, indicated by the N···O intermolecular separation, shows a linear trend upon compression, with a comparable compression rate $\partial d/\partial P = -0.031 \pm 1 \times 10^{-3}$ Å GPa^{-1} up to 6 GPa, after which the slope becomes almost zero. At 10.3 GPa the N···O distance has shortened from 2.9 to 2.6 Å (Table S1†).

The intramolecular bond lengths gradually decrease up to 4 GPa. Above this pressure there is a sudden elongation of the bonds upon further compression (Fig. 3). The changes in bond length are accompanied by changes in bond and torsion angles that indicate a flattening of the molecule (Fig. 3). This flattening enables a tighter packing of the molecules.[8] Taken together these data suggest that a structural transformation has taken place. The high pressure crystalline form will be referred to as the β-form and the low pressure structure will be called the α-form. A refinement of a pattern of the β-form at 10 GPa is shown in Fig. S1.† The corresponding representations of both the α and β polymorphs are compared in Fig. 4. As a result of the compression, the isopropyl groups rotate with respect to the a-axis allowing a more efficient packing of the molecules in the crystal lattice. Table S2† highlights the main differences in the structural parameters of these two phases. It is noteworthy that NiPPA remains crystalline up to the highest pressure. Many molecular systems undergo amorphization when compressed.[2] Lewicki *et al.* have suggested that the presence of hydrogen bonds might be at the origin of this lack of amorphization.[7]

The bulk modulus (K_0) was obtained by the Birch–Murnaghan equation of state, with K' constrained to 4, to the volume data (Fig. 2).[25] The calculated K_0 of 1.5 GPa is rather low, indicating that this is a highly compressible material. This is mainly due to the compressibility of the crystal along the a axis that corresponds to the spacing between the NiPPA-sheets.
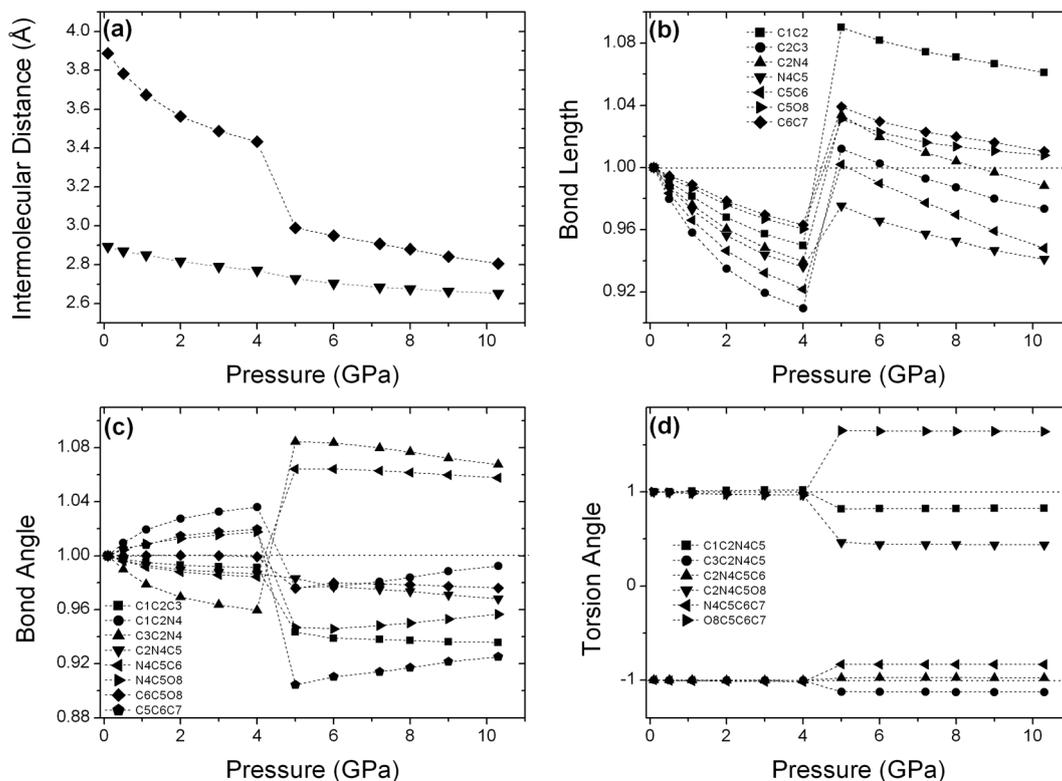
Fig. 3 Selected intermolecular distances (a), bond lengths (Å) (b), bong angles (c) and torsion angles (°) (d) of the crystalline phase of NiPPA upon compression. The intermolecular distances shown in (a) correspond to O⋯O distance along the *a*-axis (♦) and N⋯O distance along the *c*-axis (▼). Normalised values are used, except in (a).

Upon decompression the peak shifts are found to be reversible down to 100 MPa (Fig. 1). Below this pressure, the crystalline phase transforms into the plastic crystalline structure (*vide infra*). Non-hydrostatic runs were performed with no clear differences observed in the pressure behaviour of the crystalline NiPPA structure with respect to the hydrostatic experiments.

Pressure–temperature phase diagram

A set of *P*,*T* runs was carried out in order to explore the stability ranges of the crystalline and plastic crystalline NiPPA phases (Fig. 5). A simple setup was built using a regular DAC provided with three thermocouples along the path of a hot air stream provided by a jet furnace. The three thermocouples are attached, respectively, at the rear end of the DAC (close to the jet output), near the diamond anvils in the centre of the DAC, and at the far end of the DAC on the other side of the anvils. The diffraction patterns under different *P*, *T* conditions were obtained when the temperature readings from the three thermocouples were stabilised within ±1 °C of each other.

In a first run at 294 K, the compression of NiPPA to 8.0 MPa resulted in a gradual transformation from the plastic crystalline phase into the crystalline structure (Fig. 5, run 1). Some of the patterns obtained during this transformation showed coexistence of these two phases associated with the

kinetics of the first order transition. A similar phase coexistence phenomenon has been observed in the case of cyclopentane and 2,2-dichloropropane.[17,26] Once the pressure reached 44 MPa a temperature ramp was initiated. The pressure increased gradually as a result of the heating, reaching 1384 MPa at 302 K. The XRD peak positions shifted due to the compressibility and thermal expansion parameters, and peak broadening occurred, but the characteristic crystalline pattern was still recognisable. However, all crystalline reflections disappeared at 348 K, marking the melting point of the compound in this pressure range. An abrupt pressure drop was recorded indicating that the volume change on melting is negative, at least in this low pressure range. We observed that the diffraction pattern corresponding to the plastic crystalline (PC) phase always appeared rapidly just before the melting event. This indicates that the PC phase occupies a narrow field in *P*–*T* space just before the onset of melting. The C–PC transition must occur somewhere in the range indicated by a shaded area in our preliminary phase diagram (Fig. 5). The molten sample generally re-crystallized as the PC phase upon cooling to ambient conditions.

Re-crystallization of the sample was not always observed, however. In one run, the crystalline sample was initially pressurised to 120 MPa and then heated in steps to 355 K causing the pressure to increase first to 250, then to 300 and finally 365 MPa (Fig. 5, run 2). The sample remained in the C phase throughout. However, further heating resulted in rapid
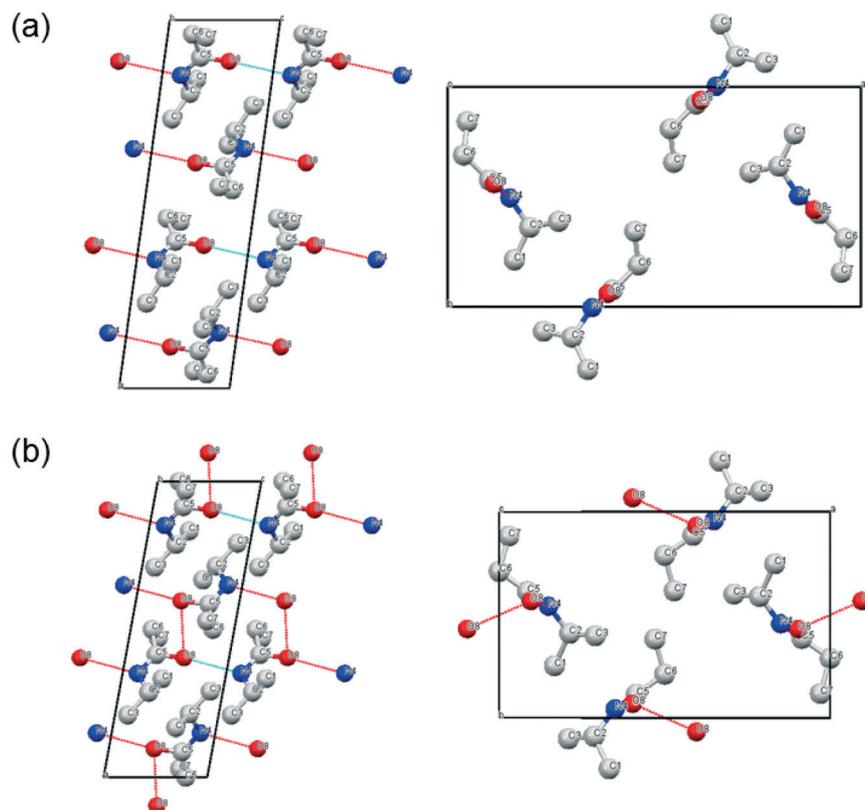
Fig. 4 Crystal structure of the crystalline phase of NiPPA at 4 GPa (α-form) (a) and 5 GPa (β-form) (b) at 293 K; view along the *b* axis (left) and along the *c* axis (right). Colour code: carbon atoms (grey), nitrogen atoms (blue) and oxygen atoms (red).
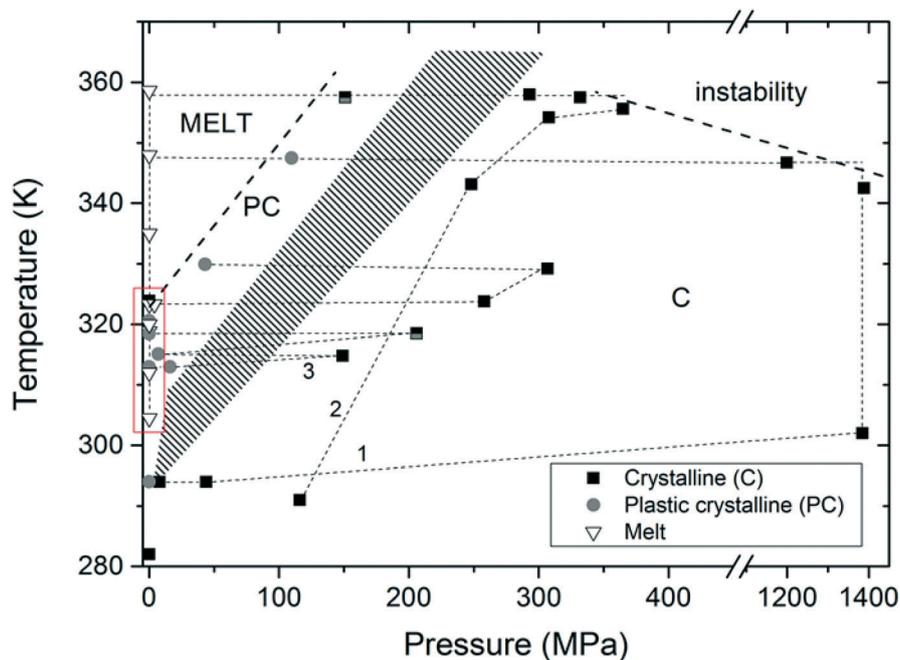

Fig. 5 Diagram illustrating the *P–T* paths (1, 2 and 3: dotted lines) followed to investigate the phase transformation behaviour of NiPPA. The area highlighted in red shows the disruption of the compound following high-*P,T* treatment in run 2 (see text for details). Note that the plastic crystalline phase is metastable at all *P,T*-values. The shaded region indicates the area in which a metastable C–PC phase transition is expected to occur. The dashed line at top right indicates the presence of a crystalline instability that results in rapid loss of pressure from the cell and disappearance of the X-ray diffraction pattern.

drop in pressure to a near-ambient value, along with disappearance of the crystalline diffraction peaks. This behaviour is similar to that observed during melting at lower pressure, although no PC or C diffraction peaks could be observed following cooling to ambient conditions, even several hours after decompression. Similar behaviour was recorded for a sample compressed to 1400 MPa and then heated (Fig. 5). A first hypothesis suggests that this behaviour is associated with a melting event as observed below 150 MPa. However, that would require a dramatic change in slope of the melting line, and adjustment of the C–PC-melt relations. We attempted to investigate the phenomenon more closely by following a third P–T path (Fig. 5, run 3). A sluggish PC–C transition was observed during compression up to 149 MPa at 314 K, with observation of patterns that indicated the metastable coexistence of these two phases. The sample was returned to ambient conditions and compressed again at 318 K. It was now observed that the plastic crystalline phase could be quenched and that the PC and C phases co-existed at 200 MPa. The crystalline structure was still present upon decompression at 318 K, but it quickly transformed into the PC phase at 320 K, melting at 324 K at ambient pressure. Interestingly, the slow growth of a single crystal was optically observed in the DAC under these conditions. The PC–C transition was observed to occur again upon compression to 260 MPa at 324 K. The crystalline phase was always present during decompression from 300 to 50 MPa at 329 K, before finally transforming back into the PC phase upon cooling to 320 K. When cooling NiPPA at a rate of 1 °C min^{-1} at ambient pressure, the PC phase transformed into the plastic crystalline structure at ~258 K. However, it was possible to quench the plastic phase below the plastic–crystalline transition temperature by cooling at higher rates (10 K min^{-1}).[15] Likewise, it was possible to quench the plastic crystalline phase beyond its stability region with sudden pressure jumps, albeit a highly disordered version of the structure as evidenced by a very dramatic intensity drop and broadening of all reflection peaks in the XRD patterns (Fig. S2†). Once quenched at extreme pressures, the plastic crystalline phase did not transform into the crystalline structure when maintained at 12 GPa for 12 hours in non-hydrostatic conditions. The shift of a few reflection peaks could be followed up to 12.2 GPa (Fig. S2†). This phase seems to be thermodynamically stable below 100 MPa in the range 300–320 K. Outside this region the crystalline phase is stable at high pressures and temperatures as high as 360 K. Nevertheless, the plastic crystalline phase is frequently observed before the melting of the crystalline phase.

The resulting data have been collected together to provide some preliminary observations concerning the NiPPA P,T phase diagram (Fig. 5). However, it is apparent that kinetic effects associated with the appearance or persistence of metastable molecular conformations and H-bonded patterns must play a role in determining the complex nature of the observed phase relations. In the case of cyclopentane the co-existence of plastic and crystalline phases was also found to

occur over a pressure range rather than at a sharp transition pressure, during both compression and decompression, clearly indicating the presence of non-equilibrium effects.[18] It is apparent that the PC configuration is thermodynamically metastable with respect to the crystalline phase at all or most P,T-conditions.

With these aspects in mind it is possible to rationalise several aspects of the diagram. First, the phase relations are similar to those of other molecular systems that adopt a plastic crystalline phase.[19,20] The plastic crystalline–liquid and crystalline–plastic crystalline phase boundaries typically run subparallel to each other, and that is possible within the constraints of the NiPPA diagram developed in Fig. 5. Very often one observes an increase in temperature stability of the PC phase with increasing pressure,[19,26] although n-alkanes provide known exceptions.[26] Fitting a straight line to the points along the PC-liquid boundary yields a melting slope (dT_m/dP) of 0.26 K MPa^{-1}, which is in good agreement with previously determined values for tert-butyl alcohols and 2-Br-adamantane, as well as related phase transitions with a an average around 0.35 K MPa^{-1}.[17,19]

Assuming a similar slope for the crystalline–plastic crystalline boundary as for the plastic crystalline–liquid boundary, using the Clausius–Clapeyron equation and inserting the value of dT_m/dP as well as the melting entropy for the crystalline to plastic crystalline phase transition at ambient pressure determined previously (17.84 J K^{-1} mol^{-1}),[15] one can calculate an apparent volume change (ΔV_{app}) as well as an apparent enthalpy change (ΔH_{app}) associated with this transition. The respective values are +4.6 cm^3 mL^{-1} and 5.05 kJ mol^{-1}. These values are similar to those reported for other C–PC transitions as in the case of tert-butylamine (+4.9 cm^3 mL^{-1} and 5.6 kJ mol^{-1}) and 2,2-dimethylpropane (+9.08 cm^3 mL^{-1} and 2.35 kJ mol^{-1}).[19,20] Interestingly, the presence of hydrogen bonds does not seem to give rise to any difference in the apparent thermodynamic parameters (ΔV and ΔH) compared to non-hydrogen bonded systems. Presumably, in this case, this is due to the fact that the hydrogen bonds remain present and in comparable concentration in all phases.[15]

A second observation is that the crystalline phase exhibits an instability that causes the pressure inside the cell to drop and the X-ray pattern disappears. This could be associated with a melting event occurring at high pressures and high temperatures. That would require a melting line with negative Clapeyron slope (dT_m/dP < 0) and the existence of a triple point in the vicinity of 200–250 MPa and approximately 360 K.

Conclusions

The P,T phase diagram of N-(isopropyl)propionamide (NiPPA) was examined over a wide pressure range. This allowed the observation of two phenomena that are usually observed in separate systems and that, to our knowledge, have not been observed before for the same molecular system: the pressure-

dependence of the plastic crystalline (PC)-crystalline (C) phase transition, which enabled the determination of the apparent volume change associated with this transition (at 0.1 MPa), and an isosymmetric transition occurring in the crystalline state at high pressure. Although NiPPA crystals contain intermolecular hydrogen bonds, the phase behaviour of the solid phases was not found to be different from that of non-hydrogen bonded molecular systems, based on thermo-dynamic analysis of the phase transformation properties. On the other hand, the presence of hydrogen bonds has been shown to influence the energy barrier for molecular rotation at atmospheric pressure,[15] suggesting that they mainly influence the dynamical behaviour of the system. Our results also emphasize the metastable nature of plastic crystalline phases and the important role of kinetics in plastic crystalline–crystalline phase transitions.

Acknowledgements

Notes and references

1 (a) F. Meersman and P. F. McMillan, *Chem. Commun.*, 2014, **50**, 766–775; (b) D. Machon, F. Meersman, M. C. Wilding, M. Wilson and P. F. McMillan, *Prog. Mater. Sci.*, 2014, **61**, 216–282.

2 F. P. A. Fabbiani and C. R. Pulham, *Chem. Soc. Rev.*, 2006, **35**, 932–942.

3 P. Wood, D. A. Haynes, A. R. Lennie, W. D. S. Motherwell, S. Parsons, E. Pidcock and J. E. Warren, *Cryst. Growth Des.*, 2008, **8**, 549–558.

4 E. V. Boldyreva, *Cryst. Eng.*, 2003, **6**, 235–254.

5 *High-Pressure Crystallography*, ed. A. Katrusiak and P. F. McMillan, Kluwer Academic Publishers, Dordrecht, 2004.

6 W. Cai and A. Katrusiak, *CrystEngComm*, 2012, **14**, 4420–4424.

7 S. Lewicki, J. W. Wasicki, L. Bobrowicz-Sarga, A. Pawlukojc, I. Natkaniec and A. Kozak, *Phase Transitions*, 2003, **76**, 261–270.

8 E. V. Boldyreva, T. P. Shakhtshneider, M. A. Vasilchenko, H. Ahsbahs and H. Uchtmann, *Acta Crystallogr., Sect. B: Struct. Sci.*, 2000, **56**, 299–309.

9 B. Wunderlich, *Thermochim. Acta*, 1999, **340–341**, 37–52.

10 P. F. McMillan, *J. Mater. Chem.*, 2004, **14**, 1506–1512.

11 W. Zieliński and A. Katrusiak, *Cryst. Growth Des.*, 2014, **14**, 4247–4253.

12 R. Brand, P. Lunkenheimer and A. Loidl, *J. Chem. Phys.*, 2002, **116**, 10386.

13 B. Geukens, F. Meersman and E. Nies, *J. Phys. Chem. B*, 2008, **112**, 4474–4477.

14 Y. Ono and T. Shikata, *J. Am. Chem. Soc.*, 2006, **128**, 10030–10031.

15 F. Meersman, B. Geukens, M. Wübbenhorst, J. Leys, S. Napolitano, Y. Filinchuk, G. Van Assche, B. Van Mele and E. Nies, *J. Phys. Chem. B*, 2010, **114**, 13944–13949.

16 C. Ma, Q. Zhou, F. Li, J. Hao, J. Wang, L. Huang, F. Huang and Q. Cui, *J. Phys. Chem. C*, 2011, **115**, 18310–18315.

17 P. Negrier, M. Barrio, J. L. L. Tamarit and D. Mondieig, *J. Phys. Chem. B*, 2014, **118**, 9595–9603.

18 S. N. Tkachev, M. Pravica, E. Kim and P. F. Weck, *J. Chem. Phys.*, 2009, **130**, 204505.

19 J. Reuter, D. Büsing, J. L. L. Tamarit and A. Würflinger, *J. Mater. Chem.*, 1997, 7, 41–46.

20 M. Barrio, P. de Oliveira, R. Céolin, D. O. López and J. L. L. Tamarit, *Chem. Mater.*, 2002, **14**, 851–857.

21 H. K. Mao, J. Xu and P. M. Bell, *J. Geophys. Res.: Space Phys.*, 1986, **91**, 4673–4676.

22 S. Rekhi, L. S. Dubrovinsky and S. K. Saxena, *High Temp. - High Pressures*, 1999, **31**, 299–305.

23 A. P. Hammersley, S. O. Svensson, M. Hanfland, A. N. Fitch and D. Häusermann, *High Pressure Res.*, 1996, **14**, 235–248.

24 J. Rodríguez-Carvajal, *Phys. B*, 1993, **192**, 55–69.

25 R. Quesada Cabrera, F. Meersman, P. F. McMillan and V. Dmitriev, *Biomacromolecules*, 2011, **12**, 2178–2183.

26 P. Negrier, L. C. Pardo, J. Salud, J. L. L. Tamarit, M. Barrio, D. O. López, A. Würflinger and D. Mondieig, *Chem. Mater.*, 2002, **14**, 1921–1929.

27 A. Würflinger, *Faraday Discuss. Chem. Soc.*, 1980, **69**, 146–156.